JOURNAL OF MATERIALS SCIENCE **34** (1999) 2335–2344

Mechanical properties of uniaxially oriented syndiotactic polystyrene

R. J. YAN*, A. AJJI‡, D. M. SHINOZAKI*
*Department of Mechanical and Materials Engineering, The University of Western Ontario, London, Canada
‡Industrial Materials Institute, NRC, Boucherville, Canada
E-mail: shinozaki@uwo.ca

Syndiotactic polystyrene has been oriented by uniaxially drawing at temperatures near the glass transition temperature, starting with amorphous material produced by quenching from the melt. The hot drawing process involves concurrent crystallization and orientation. Increasing crystallinity by itself does not affect the mechanical properties to any large extent. The orientation process is shown to substantially increase the strength and modulus in the draw direction. The anisotropy of mechanical properties is compared to mathematical models: the modulus using Arridge's model for oriented block copolymers, and the tensile strength using both the Hill-von Mises yield criterion and a modified fiber composite analog.

1. Introduction

Syndiotactic polystyrene (sPS) has been introduced recently as an important new commodity plastic, and is being considered for a wide variety of potential applications [1]. Of great interest is its relatively high crystalline melting point, which suggests service temperatures which are high for common plastics. It has been studied extensively in recent experimental work concerned with aspects related to its crystallization behaviour [2–6]. The microstructure and mechanical properties of injection molded and blended material have been reported [7–13]. Relatively little has been published on oriented forms [14–15], with interesting evidence that the glass transition temperature is affected by drawing [14]. The development of orientation with uniaxial drawing has been studied very recently using optical birefringence and thermal analysis [16].

Of continuing interest is the development of high strength material by orienting molecules, ultimately producing ultra-high modulus material [17]. Hot drawing is one technique which can induce some degree of orientation of the long chain molecules [18] and is attractive since it can be incorporated in industrial scale rapid processing. A considerable amount of work has been published on this topic, dealing with the crystalline commodity plastics such as polyethylene [19] and polypropylene [19–21]. The role of microstructure in affecting the anisotropy of mechanical properties has been extensively discussed in these early studies. The analysis of the anisotropy of oriented polymers has been reviewed by Ward [18].

The present work studies the development of orientation and anisotropy of mechanical properties with uniaxial hot drawing of sPS. Unlike polyethylene and polypropylene, sPS can be quenched in bulk form to a largely amorphous state. The subsequent molecular mobility limited crystallization of this precursor can be controlled because the mobility of the molecules near the glass transition can be changed with adjustments in temperature [6]. Of interest in this work was the characterization of the mechanical anisotropy and of the parameters which control its development in the temperature range near this transition.

2. Experimental

Syndiotactic polystyrene (Questra from Dow Chemical) with $M_w = 2.12 \times 10^5$ and a polydispersity of $M_w/M_n = 2.06$ were compression molded into plaques of 0.8 mm thickness. The nominal melting point was 266 °C and appropriately high temperatures were necessary to obtain defect free samples. It should be noted that the exact melting endotherm was sensitive to the prior thermal history of the sample. Quenching from the molten state produced optically transparent sheet with no observable crystalline diffraction maxima in the wide angle X-ray diffraction patterns.

The amorphous plaques could then be crystallized by free annealing, or drawn at temperatures above the glass transition. For tensile testing of anisotropic sheet, initially amorphous compression molded plaques were large enough that after uniaxial hot drawing, the reduced width specimen could still be cut into small tensile bars. The mechanical properties reported represent the average of 3 to 5 tests.

The thermal analysis data were obtained using a Perkin Elmer DSC7 differential scanning calorimeter. The crystalline content was measured using a heating rate of 80 °C/min following the procedure described by Kryzystowczyk *et al*. [22]. The rate of crystallization increases rapidly with temperature, and the high heating rate minimizes the amount of crystallization which

occurs during the heating. The relative areas under the melting and crystallization peaks could then be used to calculate the fractional crystallinity, assuming the heat of fusion for the crystalline sPS is 53.2 J/g [23].

The degree of orientation was estimated by measuring the optical birefringence:

$$\Delta n_{\mathrm{TM}} = n_{\mathrm{transverse}} - n_{\mathrm{machine}}$$

The experimental method has been previously described, and involves the fitting of the theoretical transmitted intensity spectrum (for white light), to the measured data [24, 25].

3. Results and discussion

3.1. Selection of draw temperature

Earlier work has shown that the rate of crystallization from the amorphous state increases with increasing temperature above the glass transition, reaches a maximum around 190 °C, and decreases towards the melting temperature [6].

$$k(T) = k_0 \exp\left(-\frac{U}{R(T - T_\infty)}\right)\exp\left(-\frac{A}{T\left(T_{\mathrm{m}}^0 - T\right)f}\right) \tag{1}$$

The first term represents the effect of molecular mobility, which dominates at low temperatures, near the glass transition; while the second term represents the thermodynamic driving force for crystallization, which dominates at high temperatures, near the equilibrium melting temperature. Comparison with isothermal experimental data showed that $U = 2950$ cal/mol, $A = 5.45 \times 10^5$ K^2 and $k_0 = 0.64 \times 10^8$ s^{-1}. In the present experiments, the focus was on the development of orientation near the glass transition, where crystallization occurred in a deformation field. The driving force for crystallization represented by the second term is relatively insignificant, and the kinetics are controlled by the effective viscosity in the amorphous state.

Experimentally, it was seen in the earlier work that crystallization in the absence of strain does not occur at temperatures below approximately 115 °C. This was confirmed for the material used in the present study in Fig. 1. Starting with amorphous samples, the fractional crystallinity was measured after 10 minutes at the annealing temperature, and essentially no additional crystallization was observed near the glass transition temperature (approximately 100 °C). The time scale was chosen as representative of the subsequent hot drawing experiments. Rapid crystallization on this time scale was observed at temperatures above the critical value of 130 °C, where the molecular mobility increases significantly. At the higher temperatures, crystallization is complete (55–60% is the maximum observed).

To obtain crystallization during drawing of the amorphous phase, a temperature of 107 °C was chosen, below the critical temperature but above the glass transition for PS.

3.2. Mechanical properties of isotropic partially crystalline samples

The measured dynamic mechanical storage modulus has been shown to increase by approximately 25% when amorphous (quenched) sPS is annealed to produce fully crystallized (60%) material [26]. The tensile modulus increases by a similar amount (Fig. 2a). The effective modulus of the crystalline phase may be estimated by fitting the data to the Voigt and Reuss models:

Voigt (isostrain):

$$E_{\mathrm{composite}} = E_{\mathrm{c}} V_{\mathrm{c}} + E_{\mathrm{a}}(1 - V_{\mathrm{c}})$$

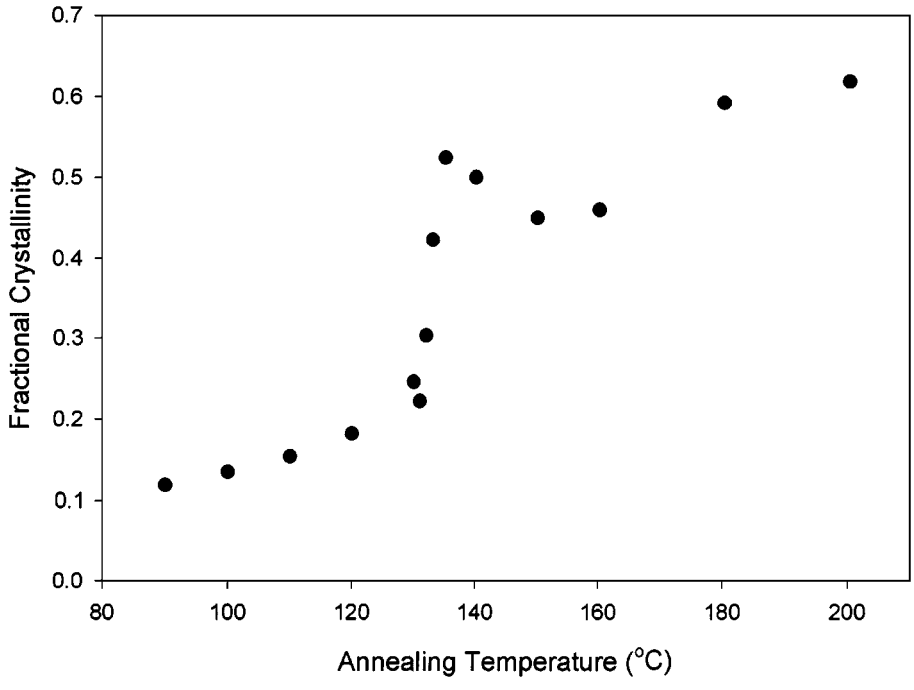

Figure 1 Crystallinity measured after 10 minutes at the indicated temperature.

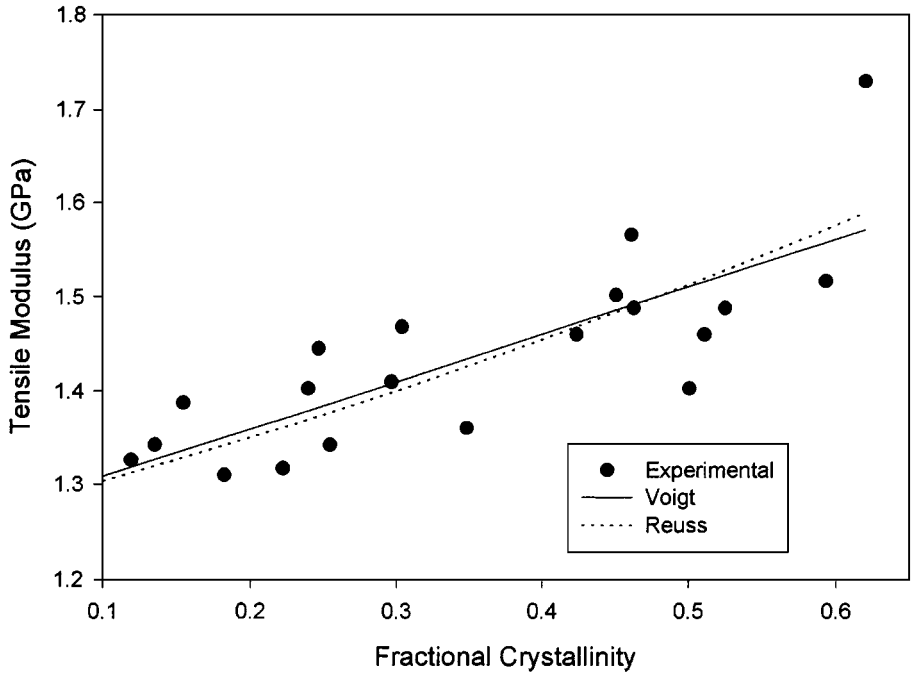

(a)

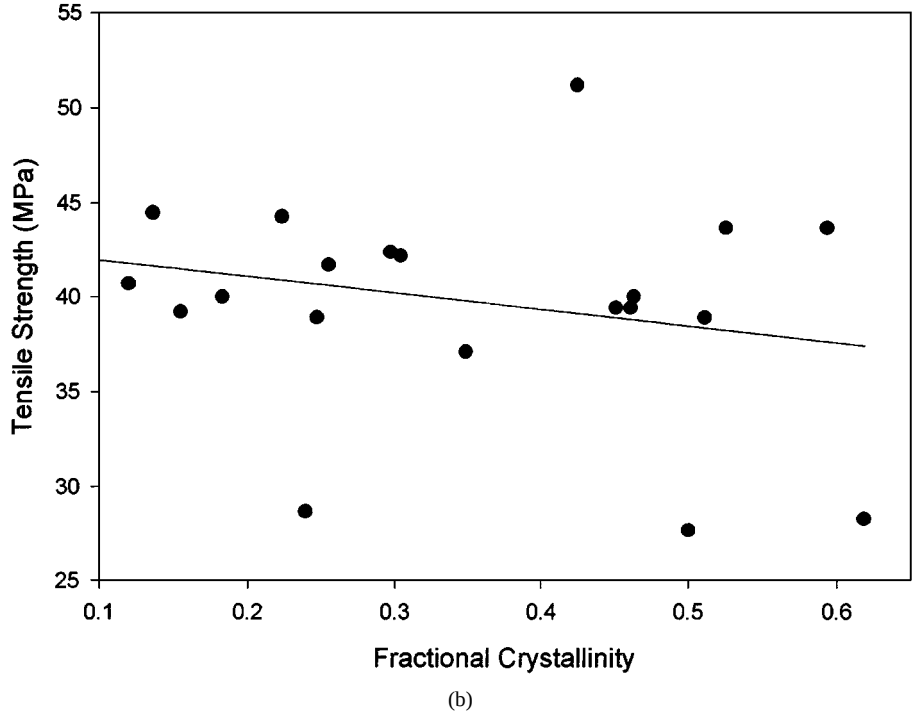

(b)

Figure 2 (a) The tensile modulus of isotropic sPS increases with crystallinity. The Voigt and Reuss models are calculated using the crystalline modulus as a fitting parameter (1.8 GPa for the Voigt and 1.9 GPa for the Reuss). (b) The tensile strength shows a large scatter. The linear regression line suggests a slight decreasing tendency as the crystallinity increases.

Reuss (isostress):

$$E_{\text{composite}} = \frac{E_a E_c}{E_c(1 - V_c) + V_c E_a}$$

where $E_{\text{composite}}$ is the average modulus of the crystalline-amorphous composite, E_a and E_c are the average moduli for the amorphous and crystalline phases. The amorphous phase modulus is estimated by measuring the tensile modulus of quenched sPS (1.3 GPa). The measured composite moduli are fitted to the two models by adjusting the crystalline modulus. The result suggests a crystalline modulus between 1.8 and 1.9 GPa. The crystalline phase is, of course, lamellar in morphology [6], and therefore elastically anisotropic. The calculated crystalline moduli are volume averages, and assume isotropy. However, at room temperature, the similarity in crystalline moduli estimated for the two models suggests that the composite modulus is insensitive to the exact elastic anisotropy of the lamellae. It should be noted that the values estimated are not very accurate, and an error of $\pm 20\%$ might be expected. Within this error band the two models show essentially the same crystalline modulus.

The tensile strength shows a large scatter (the correlation coefficient for the fitted line is 0.063) with a slight tendency to decrease as the crystallinity increases (Fig. 2b). The specimens failed in tension at relatively small strains, suggesting fracture initiation in the amorphous phase. The minimum tensile strength observed was approximately 27 MPa. The failure of low ductility material can be described in terms of the statistical distribution of flaw size, which apparently is quite wide for the quenched annealed microstructures (corresponding to a small Weibull modulus). This is expected for the randomly oriented, widely separated lamellae observed for this material [6].

3.3. Development of orientation strengthening with uniaxial drawing

The stress-strain curve shows the expected large strain hardening which develops on drawing at 107 °C (Fig. 3). At strains greater than 2.5 to 3 the material becomes significantly harder. This is noticeable at the higher strain rates. The degree of orientation increases as the material hardens (Fig. 4). At the draw rate used, a time of 12 min elapses at temperature before a draw ratio of 3 is achieved. At 107 °C, from the isotropic crystallization kinetics, no significant amount of crystallization was expected [6]. The measurement of fractional crystallinity, however, shows that the deformation

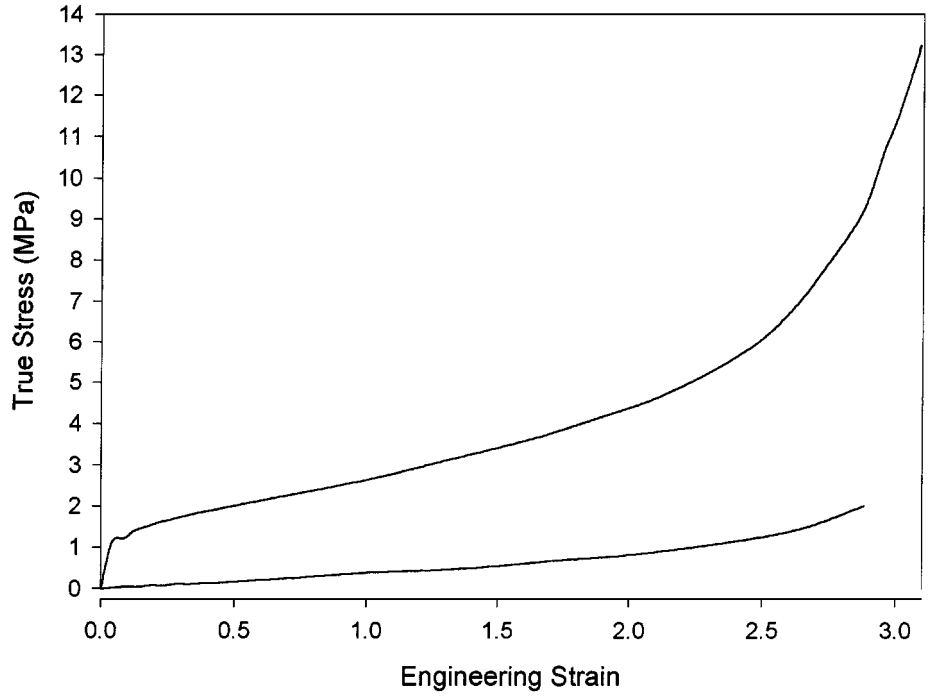

Figure 3 Tensile stress-strain curve for initially unoriented sPS at strain rates 10 min^{-1} and 0.17 min^{-1} showing the hardening at high strains.

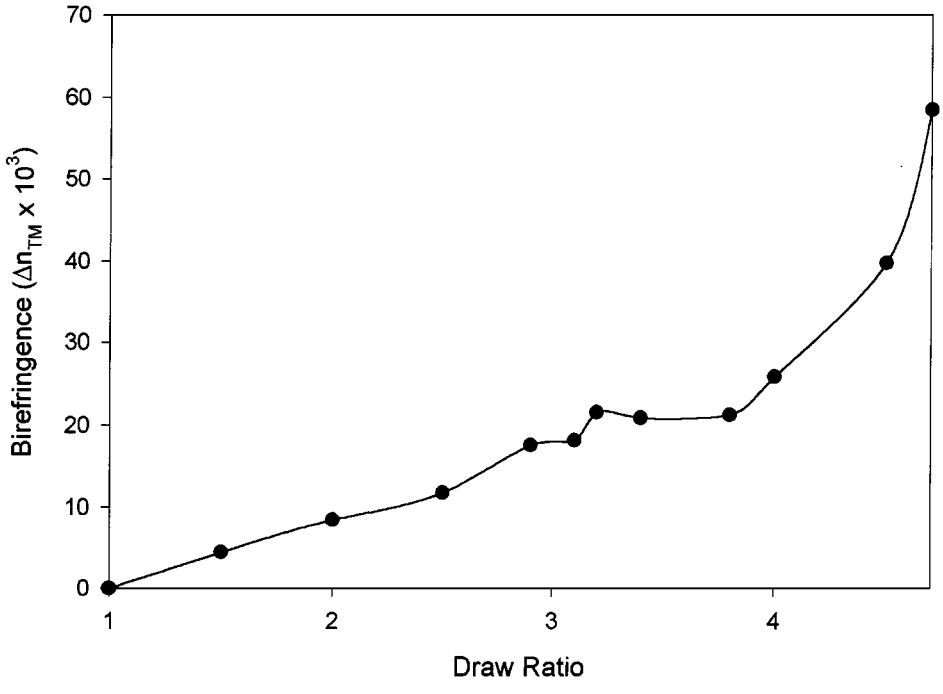

Figure 4 The optical birefringence and degree of orientation increases with increasing draw ratio (for draw rate = 0.17 min^{-1}).

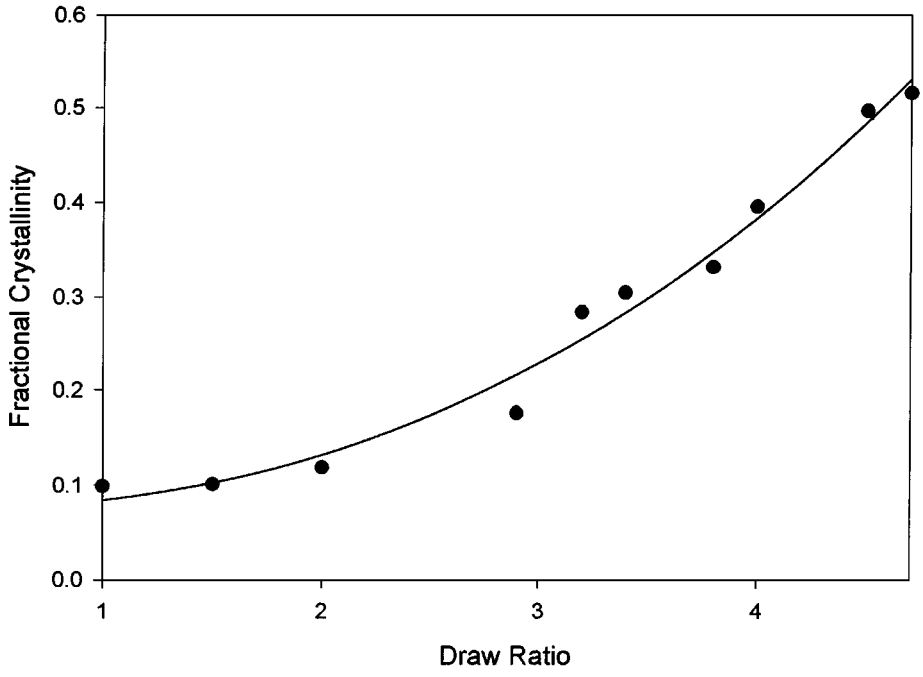

Figure 5 Draw induced crystallization at 107 °C for a draw rate of 0.17 min^{-1}. The fitted line is $y = 0.074 + 0.011x^{2.4}$, where y is the crystallinity and x is the draw ratio.

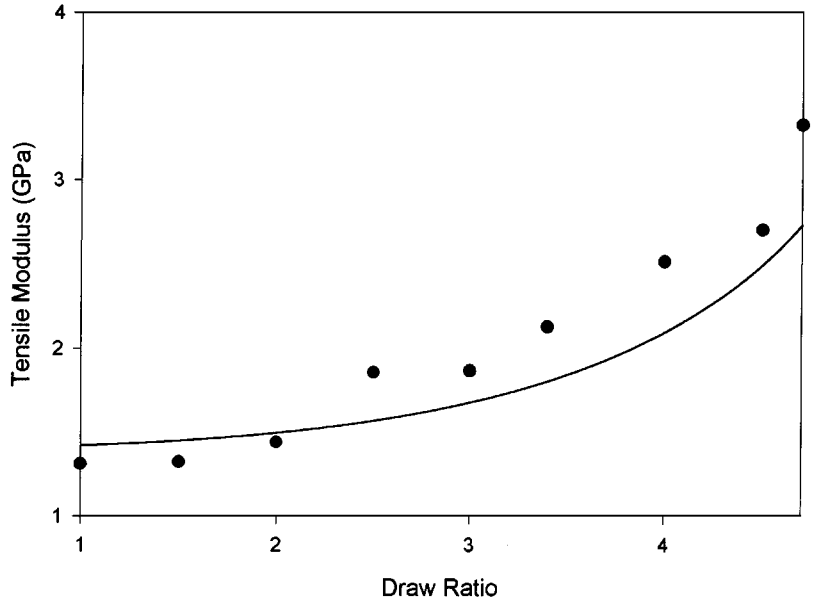

Figure 6 Longitudinal tensile modulus versus draw ratio. The series coupled (Reuss) crystalline-amorphous model is fitted to the data using the crystalline modulus as the fitting parameter. The crystallinity is obtained from the fitted line of Fig. 5. The fit shown is for a crystalline phase which is rigid (infinite stiffness).

induces crystallization, increasing rapidly above a draw ratio of 3 (Fig. 5).

Earlier studies of drawing using X-ray diffraction showed that the crystalline unit cell was oriented with the molecular axis preferentially aligned parallel to the draw direction [16]. Electron microscopy of quenched and annealed sPS shows lamellae of the classical morphology, separated by regions of amorphous material [6]. The oriented crystallization was therefore expected to result in alternating layers of lamellae and amorphous regions along the draw direction, similar to that seen in polyethylene and polypropylene. The series coupled composite therefore was expected to follow a Reuss average. The tensile modulus measured parallel to the draw direction is plotted as a function of draw ratio in Fig. 6. The crystallinity as a function of draw ratio is obtained from Fig. 5, using the fitted curve. The Reuss average model is shown as a solid line, assuming the amorphous modulus to be approximately 1.3 GPa, and fitting the crystalline modulus. The best fit gives a crystalline modulus which is at least 200 GPa. For a Reuss model, for an amorphous modulus of 1.3 GPa, at a crystalline fraction of 0.6 the maximum composite modulus expected is for an infinitely stiff crystalline fraction. The strain is carried completely by the amorphous fraction and the composite modulus is $E_a/0.4 = 3.25$ GPa. With only the crystalline modulus as a fittable parameter, the predicted modulus cannot

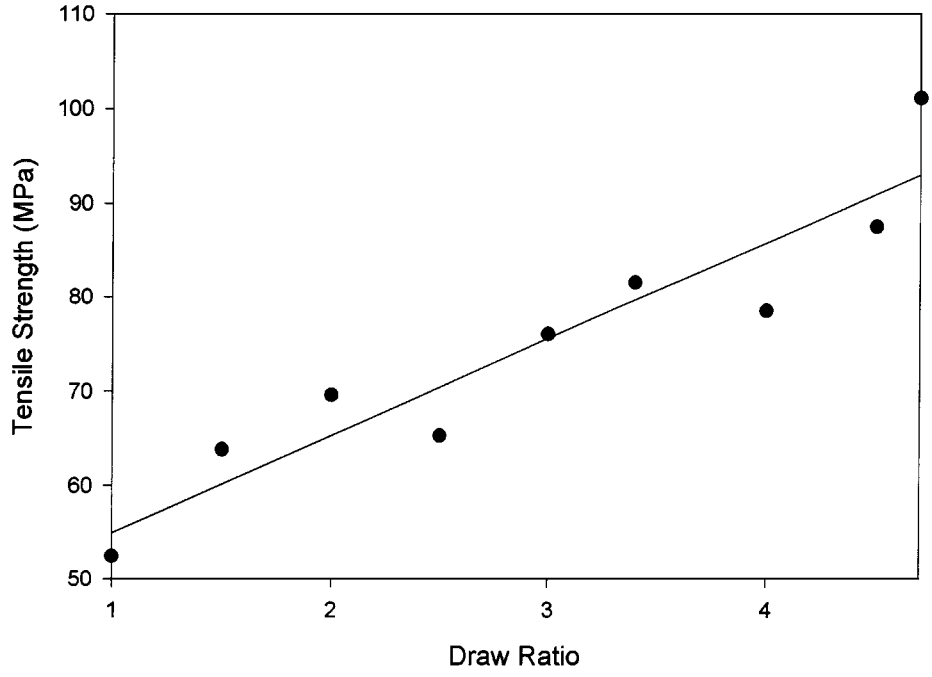

Figure 7 The longitudinal tensile strength increases linearly with draw ratio.

be increased to fit more closely to the experimental data than shown in Fig. 6. This suggests the amorphous fraction may have a higher modulus or there is physical constraint of the amorphous fraction (26) in drawn sPS.

The room temperature tensile strength increases with draw ratio (Fig. 7). This is surprising in view of the large scatter in the tensile strength of isotropically crystallized sPS (Fig. 2b), with no indication of any dependence of strength on crystallinity. The data for drawn material is clearly less scattered (correlation coefficient for the fitted line is 0.88) suggesting a lower sensitivity to random flaws, or higher Weibull modulus, and shows a significantly larger strength compared to the isotropic solid. This suggests that the oriented material is tougher, which is confirmed by the slightly higher ductilities observed in the tensile tests, and by qualitative evaluation.

3.4. Orientation and modulus

Fig. 8 shows the relationship between the measured optical birefringence and the tensile modulus parallel to the draw direction for a variety of specimens drawn under different conditions (draw temperature, ratio and rate). For a given modulus, the degree of optical orientation varies, above a modulus of 2 GPa (the point A).

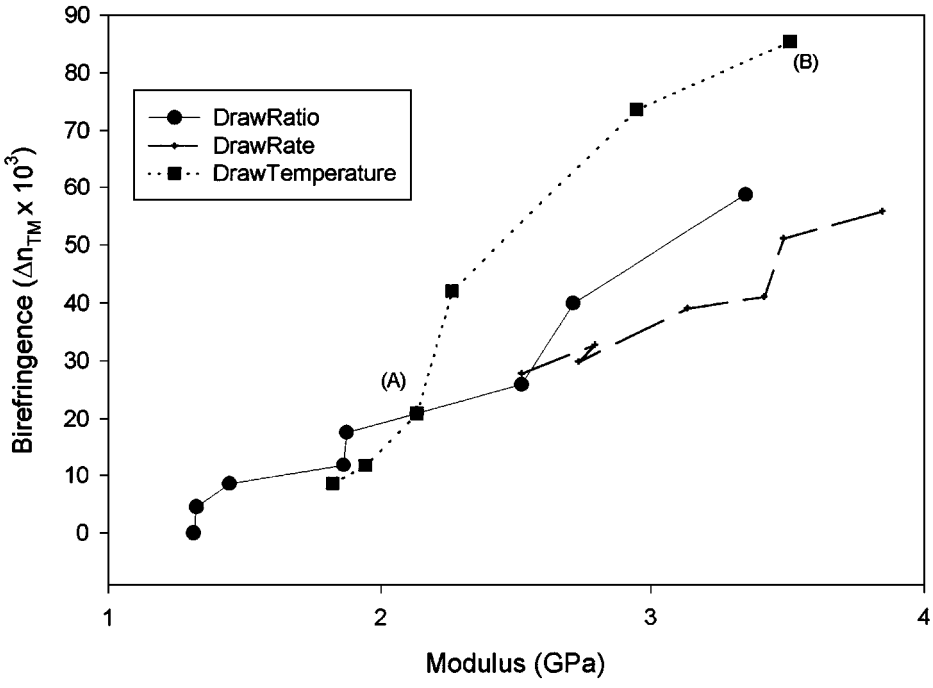

Figure 8 Optical birefringence versus modulus for 3 sets of tests varying with: draw ratio, draw rate and draw temperature. The degree of orientation is not a single valued function of modulus.

Decreasing the draw temperature from 107 °C at (A), to 90 °C at (B) on the data measured with different draw temperatures results in a higher degree of orientation, and a resultant higher modulus. However the latter temperature is well below the glass transition where the molecular mobility is very low. Comparison of material with similar moduli obtained at higher draw ratio at 107 °C (curve 1) and at higher draw rate (curve 2), shows that the high modulus at (B) obtained by drawing at 90 °C is due to amorphous phase stretching rather than lamellar orientation. This implies that to obtain a high degree of lamellar orientation, the material should be drawn above its glass transition temperature, at relatively high draw rates to high draw ratio. However if the draw temperature is too high, the degree of orientation and modulus remain low, similar to the isotropic case.

The temperature of 107 °C used extensively in these experiments therefore appears to be close to the optimal for the strain rates obtainable in the tensile testing machine. It is likely that for industrial scale processing, where strain rates can be much higher, a higher temperature can be used.

3.5. Anisotropy of elastic properties in drawn material

Uniaxially hot drawn crystalline polymers are similar mechanically to unidirectionally oriented fiber composites, in which the longitudinal properties are larger than the transverse. Fiber symmetry dictates isotropy in the plane perpendicular to the draw direction. Arridge has analyzed this kind of elastic anisotropy in extruded block copolymers, in which the microstructure consisted of polystyrene cylinders embedded in a polybutadiene matrix: the longitudinal axis of the cylinders being the stiff direction [27, 28]. The measured tensile modulus varied with direction with respect to the longitudinal axis according to:

$$E^{-1} = S_{11}\sin^4\theta + (2S_{13} + S_{44})\sin^2\theta\cos^2\theta + S_{33}\cos^4\theta \quad (2)$$

where S_{11}, S_{13}, S_{33} (longitudinal direction), and S_{44} are terms in the compliance matrix S_{ij}, and θ is the angle between the tensile axis and the longitudinal (high stiffness) direction.

Fig. 9 shows the fit of the above function to the measured tensile modulus, using the compliances as the fitting parameters. The values for the compliances are:

$$S_{11} = 1.72 \times 10^{-9}\ \mathrm{N^{-1}\,m^2}$$
$$S_{33} = 0.36 \times 10^{-9}\ \mathrm{N^{-1}\,m^2}$$
$$(2S_{13} + S_{44}) = 1.36 \times 10^{-9}\ \mathrm{N^{-1}\,m^2}$$

which are consistent with a moderate degree of elastic anisotropy. It is notable that the model fits very well over all orientations.

For a sample which is drawn at a much slower rate at the same temperature, the degree of orientation is much lower (Fig. 10), and the best fit gives:

$$S_{11} = 0.66 \times 10^{-9}\ \mathrm{N^{-1}\,m^2}$$
$$S_{33} = 0.47 \times 10^{-9}\ \mathrm{N^{-1}\,m^2}$$
$$(2S_{13} + S_{44}) = 0.99 \times 10^{-9}\ \mathrm{N^{-1}\,m^2}$$

The compliance parallel to the draw direction (S_{33}) is about 30% higher than for the sample drawn at higher rate, as expected for the lower degree of orientation. In addition, it is interesting to observe that the transverse compliance is much higher in the more highly oriented sample. The amorphous (low stiffness) phase orients

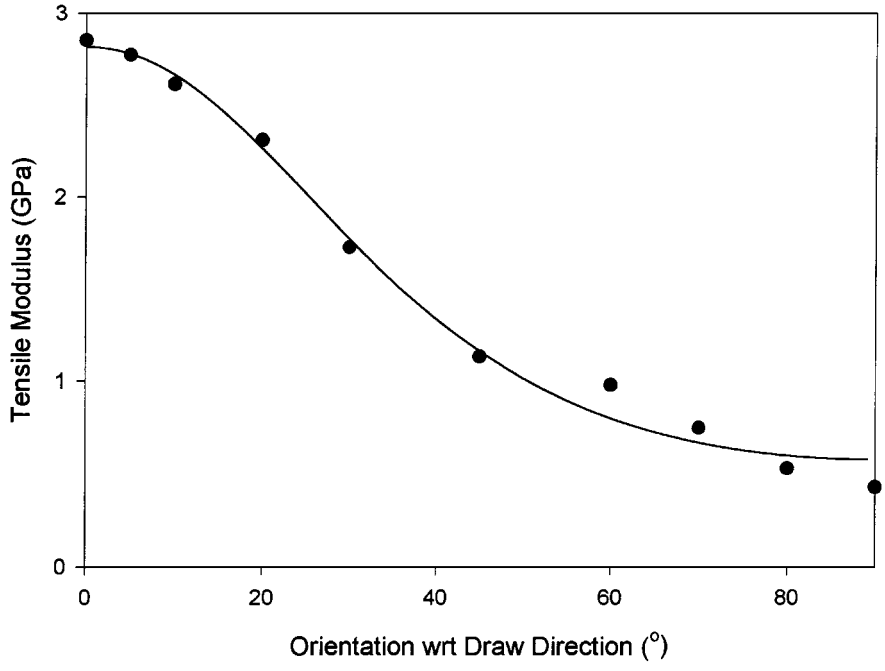

Figure 9 Anisotropy of tensile modulus for samples drawn at high rate (10 $\mathrm{min^{-1}}$). The fitted line uses Equation 2 based on Arridge's model.

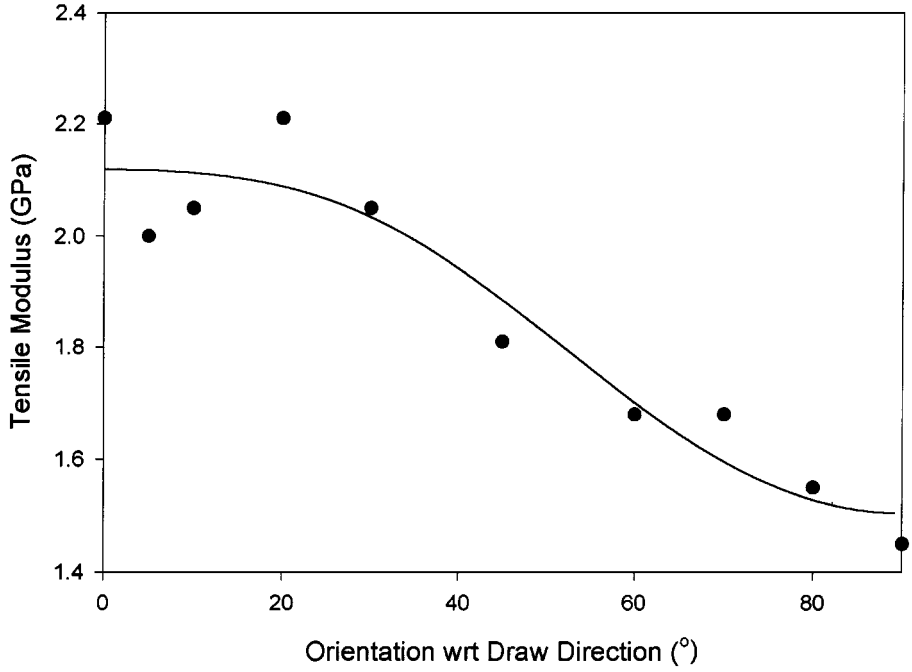

Figure 10 Anisotropy of tensile modulus for samples drawn at low rate (0.17 min^{-1}). The fitted line uses Equation 2.

in parallel to the crystalline phase, and the transverse stiffness decreases. The uniaxial orientation induces a transversely softer material. This is manifested experimentally as an increasing toughness, or decreasing sensitivity to flaws, mentioned earlier.

3.6. Anisotropy of plastic properties

The tensile strength shows an anistropy which is higher with higher draw rate (Fig. 11). The data have been fitted to the Hill-von Mises yield criterion [29].

$$\sigma_{\text{yield}} = \{(G+H)\cos^4\theta + (H+F)\sin^4\theta + 2(N-H)\sin^2\theta\cos^3\theta\}^{-1/2} \quad (3)$$

where $(G+H) = 1/X^2$, $(H+F) = 1/Y^2$ and $(F+G) = 1/Z^2$ with X, Y and Z being the tensile yield stresses along three principal directions of anisotropy for a sample with orthotropic symmetry. For fiber symmetry, the longitudinal (draw) direction is X and the transverse

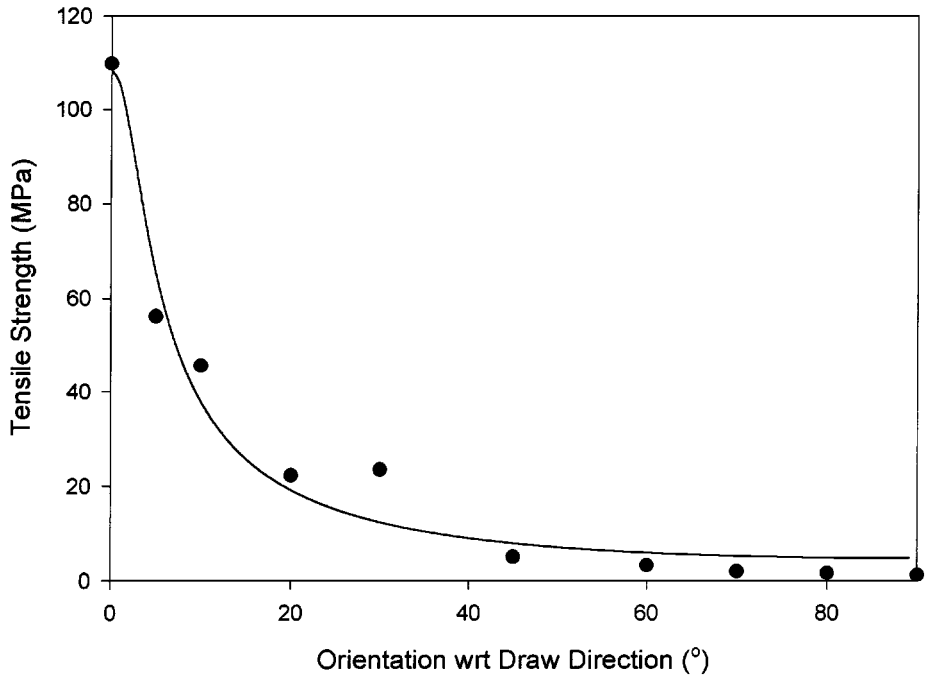

Figure 11 Anisotropy of tensile strength for samples drawn at high rate (10 min^{-1}). The fitted line uses Equation 3 based on the Hill-von Mises yield criterion.

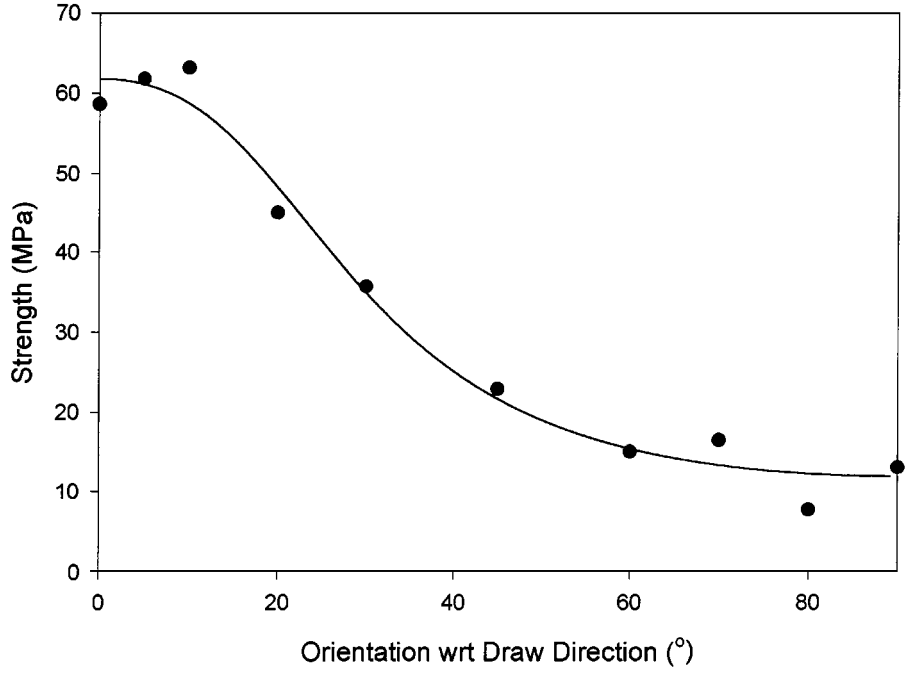

Figure 12 Anisotropy of tensile strength for samples drawn at low rate (0.17 min^{-1}). The fitted line uses Equation 3.

yield strengths are $Y = Z$. The best fit gives:

$$(G + H) = 8.5 \times 10^{-5}\ \text{MPa}^{-2}$$
$$(H + F) = 4.2 \times 10^{-2}\ \text{MPa}^{-2}$$
$$(N - H) = 1 \times 10^{-4}\ \text{MPa}^{-2}$$

For a slower draw rate, and consequent lower degree of orientation, the parameters for the best fit yield (Fig. 12):

$$(G + H) = 2.6 \times 10^{-4}\ \text{MPa}^{-2}$$
$$(H + F) = 7.0 \times 10^{-3}\ \text{MPa}^{-2}$$
$$(N - H) = 6.3 \times 10^{-4}\ \text{MPa}^{-2}$$

The transverse yield stress decreases with increasing orientation, to about 4.9 MPa, compared to 12 MPa for the less well oriented sample. However, although the fit of the function to the experimental data is good, the observed plastic strains in the transverse directions do not match the predictions from the Hill-von Mises model [30].

An alternative method to analyze the anisotropy of tensile strength is to consider a fiber composite analog model suggested earlier [30] and based on work by Kelly and Davies [31] (Fig. 13). In this model, the maximum tensile strength depends on the mechanism of failure of the oriented material, which changes with orientation. Each failure process function can be independently fitted to the experimental

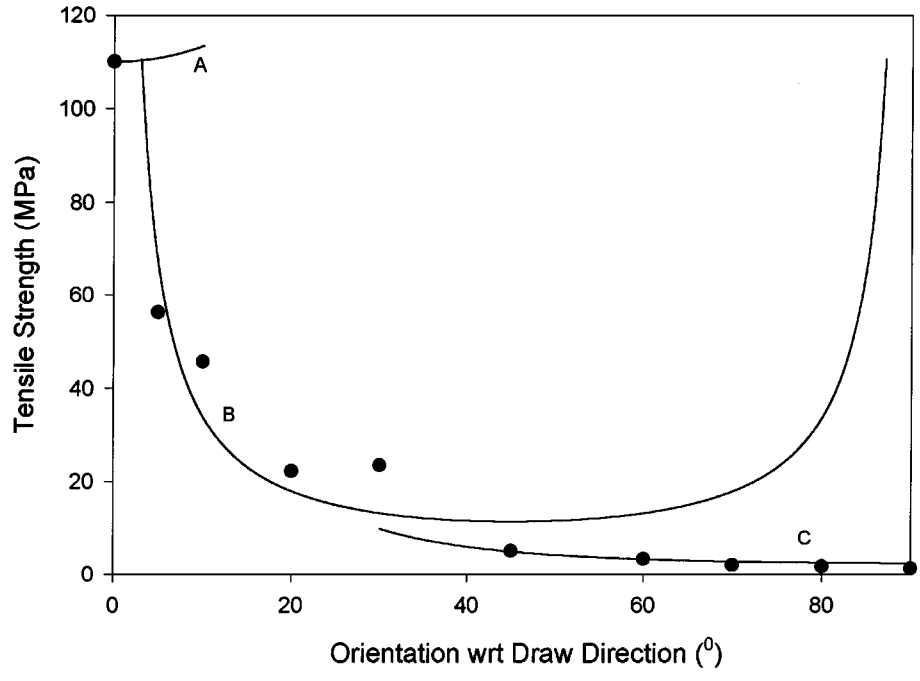

Figure 13 Tensile strength data from Fig. 11 are fitted to the fiber composite failure model, invoking three different failure criteria A, B and C.

data over the appropriate limited range of orientations.

In the region near $\theta = 0^\circ$, the "fibers" fail transversely, following the failure criterion:

$$\sigma_{\text{failure}} = \frac{\sigma_{c1}}{\cos^2 \theta} \tag{4}$$

where $\sigma_{c1} = 110$ MPa is the failure stress parallel to the orientation direction. This is seen as curve A in Fig. 13.

Over the intermediate range, the material fails by shear parallel to the orientation direction, similar to a critical resolved shear stress criterion for single crystal metals:

$$\sigma_{\text{failure}} = \frac{\tau_c}{\sin \theta \cos \theta} \tag{5}$$

where $\tau_c = 5.8$ MPa is the critical shear stress acting parallel to the draw direction at failure (curve B).

Close to $\theta = 90^\circ$, the material fails by fracture on planes parallel to the orientation direction, delaminating along planes of weakness:

$$\sigma_{\text{failure}} = \frac{\sigma_{c2}}{\sin^2 \theta} \tag{6}$$

where $\sigma_{c2} = 2.5$ MPa is the failure stress perpendicular to the orientation direction (curve C).

The usefulness of this kind of model lies principally in its close relationship to the observed failure processes which change with orientation, and therefore in estimating the range of orientations over which each mechanism is expected to dominate. In Fig. 13, the superposition of these three independent failure criteria is shown. At a given orientation, the failure process with the lowest critical stress operates. For small θ, failure occurs by fracture transverse to the orientation direction (across the molecular axis) following Equation 4, while at large θ the material fractures on planes parallel to the orientation direction, following Equation 6. Over the middle range of orientations, where the resolved shear stress is relatively high, the specimen fails by shear along planes parallel to the orientation direction (Equation 5).

4. Conclusions

The development of anistropy in uniaxially hot drawn sPS has been studied. The hot drawing in the temperature range near the glass transition was examined for material which started as almost fully amorphous. By crystallizing as the specimen was being deformed, oriented material was produced. The longitudinal mechanical properties were correlated with the degree of orientation and crystallinity. The anisotropy of mechanical properties were measured using tensile tests on specimens cut from various angles with respect to the original draw direction. The elastic anistropy followed the mechanical model proposed by Arridge for uniaxially oriented block copolymers, while the plastic anisotropy was most usefully described by a fiber composite analog. The advantage of using the latter model to describe the plastic anisotropy was that the failure mechanism was explicitly described over three ranges of orientation.

Acknowledgements

This work has been funded by the Natural Sciences and Engineering Research Council of Canada (Strategic Grant). Discussions with Michel Dumoulin, Frank Maine and Bill Newson are acknowledged. The staff of the NRC Industrial Materials Institute has helped considerably in the experiments.

References

1. D. BANK and R. BRENTIN, *Plast. Technol.* **6** (1997) 52.
2. E. J. C. KELLAR, C. GALIOTIS and E. H. ANDREWS, *Macromolecules* **29** (1996) 3515.
3. M. KOBAYASHI and T. NAKAOKI, *ibid.* **22** (1989) 4377.
4. V. PETRACCONE, F. AURIEMMA, F. DAL POGGETTO, C. DE ROSA, G. GUERRA and P. CORRADINI, *Makromol. Chem.* **194** (1993) 1335.
5. C. MANFREDI, G. GUERRA, C. DE ROSA, V. BUSICO and P. CORRADINI, *Macromolecules* **28** (1995) 6508.
6. S. ST. LAWRENCE and D. M. SHINOZAKI, *Polym. Eng. Sci.* **37**(11) (1997) 1825.
7. M. A. JONES, C. J. CARRIER, M. T. DINEEN and A. M. BALWINSKI, *J. Appl. Polym. Sci.* **64** (1997) 673.
8. S. WU, A. BUBECK and C. J. CARRIER, *ibid.* **62** (1996) 1483.
9. A. M. EVANS, E. J. C. KELLAR and J. KNOWLES, *Polym. Eng. Sci.* **37**(1) (1997) 153.
10. J. D. BARNES, G. B. MCKENNA, B. G. LANDES, R. A. BUBECK and D. BANKS, *ibid.* **37**(9) (1997) 1480.
11. H. ERMER, R. THOMANN, J. KRESSLER, R. BRENN and J. WUNSCH, *Macromol. Chem. Phys.* **198** (1997) 3639.
12. M. BONNET, M. BUHK, G. TROGNER, K.-D. ROGAUSCH and J. PERTERMANN, *Acta Polymer* **49** (1998) 174.
13. B. K. HONG, W. H. JO, S. C. LEE and J. KIM, *Polymer* **39**(10) (1998) 1793.
14. F. DE CANDIA, G. ROMANO, R. RUSSO and V. VITTORIA, *Colloid. Polym. Sci.* **268** (1990) 720.
15. C. M. HSIUNG and M. CAKMAK, *Inter. Polym. Proc.* **7**(1) (1992) 51.
16. R. J. YAN, A. AJJI and D. M. SHINOZAKI (1998) (in preparation).
17. A. CIFERRI and I. M. WARD, "Ultra-high Modulus Polymers" (Applied Science Publishers, London, 1977).
18. I. M. WARD, "Mechanical Properties of Solid Polymers" (Wiley, New York, 1983).
19. I. L. HAY and A. KELLER, *J. Mater. Sci.* **2** (1967) 538.
20. D. M. GEZOVICH and P. H. GEIL, *ibid.* **6** (1971) 509.
21. D. W. HADLEY, in "Structured and Properties of Oriented Polymers," edited by I. M. Ward (Wiley, New York, 1975).
22. D. H. KRZYSTOWCZYK, X. NUE, R. D. WESSON and J. R. COLLIER, *Polym. Bull.* **33** (1994) 109.
23. J. R. PASTOR, B. G. LANDES and P. J. KARJALA, *Thermochim. Acta* **177** (1991) 187.
24. A. AJJI, J. GUEVREMONT, R. G. MATTHEWS and M. M. DUMOULIN, SPE Antec'98 Preprints, Atlanta, GA, 1998.
25. F. BEEKMANS and A. P. DE BOER, *Macromolecules* **29** (1996) 8726.
26. S. ST. LAWRENCE and D. M. SHINOZAKI, *J. Mater. Sci.* 1998, in press.
27. R. G. C. ARRIDGE, "Introduction to Polymer Mechanics" (Taylor and Francis, London, 1985).
28. R. G .C. ARRIDGE and M. J. FOLKES, *J. Phys. D: Appl. Phys.* **15** (1982) 344.
29. R. HILL, "The Mathematical Theory of Plasticity" (Oxford University Press, Oxford, 1950).
30. D. M. SHINOZAKI and G. W. GROVES, *J. Mater. Sci.* **8** (1973) 71.
31. A. KELLY and G. J. DAVIES, *Met. Rev.* **10** (1965) 1.

Received 21 October
and accepted 16 November 1998